

# Quenched and Partially Quenched Chiral Perturbation Theory for Vector and Tensor Mesons <sup>1</sup>

Chi-Keung Chow<sup>a</sup> and Soo-Jong Rey<sup>b,c</sup>

*Newman Laboratory for Nuclear Studies  
Cornell University, Ithaca NY 14853 USA<sup>a</sup>*

*School of Natural Sciences, Institute for Advanced Study  
Olden Lane, Princeton NJ 08540 USA<sup>b</sup>*

*Physics Department, Seoul National University, Seoul 151-742 KOREA<sup>c</sup>*

ckchow@mail.lns.cornell.edu, sjrey@phya.snu.ac.kr

## abstract

Quenched and partially quenched chiral perturbation theory for vector mesons is developed and is used to extract chiral loop correction to the  $\rho$  meson mass. Connections to fully quenched and totally unquenched chiral perturbation theory results are discussed. It is also shown that (partially) quenched perturbation theory for tensor mesons can be formulated analogously, and the chiral corrections for tensor meson masses are directly proportional to their counterparts in the vector meson sector. Utilizing this observation and non-relativistic quark model, we point out that mass difference ( $m_{a_2} - \frac{3}{2}m_\rho$ ) is “quenching-insensitive” in large- $N_c$  limit. This quantity may be used for normalization of mass scale in lattice QCD calculations.

---

<sup>1</sup> Work supported in part by NSF Grant, NSF-KOSEF Bilateral Grant, KOSEF Purpose-Oriented Research Grant 94-1400-04-01-3 and SRC-Program, Ministry of Education Grant BSRI 97-2410, the Monell Foundation and the Seoam Foundation Fellowships.

Lattice QCD simulations have reached such an impressive stage of high precision that an accuracy up to a few percent error is expected to be within a reach. Amongst such results are spectroscopy of ground state hadrons including pseudo-Goldstone mesons, baryons as well as some of the vector mesons [1, 2, 3, 4, 5, 6]<sup>2</sup>. More recently, the precision test of hadron spectroscopy on a lattice has gone beyond the ground state hadrons and has been extended, for example, to tensor or exotic mesons [8, 9, 10]. The tensor mesons are of particular interest since they are relatively clean states experimentally, much more so than scalar mesons. As such, one might hope that tensor mesons provide a good check-point on accuracy of lattice QCD simulations. Technically, the difficulty has been that gauge invariant lattice interpolating operator of tensor mesons is non-local. Dynamical evolution of such operator is far more computer-time consuming than low-lying mesons and baryons that require only local operators, hence, limits accuracy of lattice data. With the advent of recent results [9, 10], however, precision spectroscopy of the tensor mesons should become possible in the foreseeable future. Such an extension should be of importance in order to gain a more complete insight and better understanding of the nonperturbative aspects of QCD.

Simulation of full QCD on a lattice has turned out to be both time consuming and costly. Most of the simulation time is to calculate changes in the determinant of the Dirac operator of light quarks. Because of this reason, so far, lattice QCD calculations on a large-scale volume have been mainly limited to quenched (valence-quark) approximation in which gauge field configurations are summed up with the determinant of  $N_F$  light quarks  $\det^{N_F}(\mathcal{D}(A) + m)$  is replaced by unity or, equivalently,  $N_F \rightarrow 0$ . While the approximation is well suited when quark masses are heavy enough [11], extrapolation of the masses to physical, light quark masses might result in potentially significant errors. It is therefore necessary to understand how reliable the quenched approximation is and where it begins to break down. Indeed, Sharpe [12, 13] and Bernard and Golterman [14, 15] have pointed out that the quenched approximation leads to sizable errors<sup>3</sup>. If this is the case<sup>4</sup>, then one needs to understand better the errors incurred by quenched approximation before a reliable hadron spectrum is extracted.

In order to study the error introduced by the quenched approximation systematically, Sharpe has developed quenched chiral perturbation theory (Q $\chi$ PT) [12, 13], which is subsequently developed further by Bernard and Golterman [14]<sup>5</sup>. In order to cancel the effect of internal quark loops, following the method proposed by Morel [21], Bernard and Golterman have introduced the ghost quarks, which have the same masses as the standard quarks, but with opposite

---

<sup>2</sup>for up-to-date review, see [7].

<sup>3</sup>Some relevant recent investigation includes [16, 17, 18].

<sup>4</sup>For up-to-date review, see [19].

<sup>5</sup>For a pedagogical review, see [20].

statistics. Diagrams with quark loops are thus cancelled by analogous diagrams with ghost loops. The quenched approximation is achieved by introducing a ghost quark to every standard quark in the Lagrangian. Just as standard chiral perturbation theory ( $\chi$ PT) is the low energy effective theory of QCD,  $Q\chi$ PT is the low energy effective theory of this new theory of quarks and ghosts. One can then estimate the error introduced by the quenched approximation by calculating the non-analytic contributions from chiral loops, and compare them with their counterparts in standard  $\chi$ PT. If the structure of the chiral non-analyticity of a physical quantity in  $Q\chi$ PT is different from that in standard  $\chi$ PT, one will expect its extrapolation to chiral limit in quenched lattice calculations to be unreliable. From a more general point of view, standard and quenched chiral perturbation theories can be regarded as two extremes of a (discrete) spectrum of theories with different degrees of quenching. This connection is made possible in partially quenched chiral perturbation theory (PQ $\chi$ PT) [15], which is the low energy effective theory of QCD with  $n$  quarks and  $k$  ghost ( $n \geq k$ )<sup>6</sup>. Standard and quenched chiral perturbation theories are recovered by tuning  $k = 0$  and  $n$  respectively.

Since its invention,  $Q\chi$ PT has been used to study various hadrons such as Goldstone bosons [12, 13, 14], baryons [24], heavy mesons [25] and exactly soluble two-dimensional QED [26]. Recently, Booth *et. al.* [27] has formulated  $Q\chi$ PT for vector mesons. Here we will extend these works in two directions. We will formulate PQ $\chi$ PT for vector mesons and study their non-analytic singularities in chiral loop corrections. We will also show that, in the heavy mass expansion formalism, it is straightforward to generalize the chiral perturbation theory to  $2^{++}$  tensor mesons or mesons with even higher spins. The relationship of the present work to previous literature is summarized in the following table:

$J^{PC}$	$\chi$ PT	PQ $\chi$ PT	$Q\chi$ PT
$0^{-+}$	Gasser, Leutwyler[28]	Bernard, Golterman[15]	Sharpe[12, 13]
$1^{--}$	Jenkins, Manohar, Wise[29]	Chow, Rey(this paper)	Booth, Chiladze, Falk[27]
$2^{++}$	Chow, Rey[30]	Chow, Rey(this paper)	Chow, Rey(this paper)

This paper is organized as follows. In the next section, we will formulate PQ $\chi$ PT of vector mesons. We will then illustrate its application to calculate the chiral one-loop correction to  $\rho$ -meson mass in Section 3, and compare it with the results from  $Q\chi$ PT and unquenched  $\chi$ PT. Lastly, generalization to tensor mesons will be treated in Section 4.

---

<sup>6</sup> Various aspects of partially quenched QCD has been studied recently in [22, 23].

# 1 Partially Quenched QCD for Vector Mesons

In this section, we review partially quenched QCD [15] and construct chiral perturbation theory for vector mesons.

Partially quenched QCD consists of  $n$  quarks  $q_i$  and  $k$  ghost-quarks  $\tilde{q}_j$ . Quark masses  $m_i (i = 1, \dots, n)$  are completely arbitrary and the ghost-quark masses are fixed to be equal to the masses of the last  $k$  quarks, viz.  $\tilde{m}_j = m_{n-k+j}, (j = 1, \dots, k)$ . As such, partially quenched QCD contains the first  $(n - k)$  unquenched quarks and the remainder  $k$  quenched ones. The full graded chiral symmetry of the partially quenched QCD is the semi-direct product  $[\text{SU}(n|k)_L \times \text{SU}(n|k)_R] \times \text{U}(1)$ . The additional axial  $\text{U}(1)$  is broken by the QCD anomaly (for  $N_c < \infty$ ). In the notation of [15] we will refer this theory as  $\text{SU}(n|k)$ -theory. Note that  $\text{SU}(n|k)$ -theory is expected to interpolate between fully unquenched QCD described by  $\text{SU}(n|0)$ -theory and fully quenched QCD described by  $\text{SU}(n|n)$ -theory.

## 1.1 Goldstone Meson Multiplet Sector

PQ $\chi$ PT for Goldstone mesons was first studied in Ref. [15]. The summary below is just a brief sketch of their work and the reader is encouraged to the original paper for details.

Goldstone meson fields can be written as a  $(n+k) \times (n+k)$  unitary matrix field  $\Sigma$  defined as:

$$\Sigma \equiv \exp(2i\Phi/f), \quad \Phi \equiv \begin{pmatrix} \phi & \chi^\dagger \\ \chi & \tilde{\phi} \end{pmatrix}. \quad (1)$$

In terms of quarks and ghost-quarks,  $\phi \approx (q_i \bar{q}_j)$ ,  $\tilde{\phi} \approx (\tilde{q}_i \bar{q}_j)$ ,  $\chi \approx (\tilde{q}_i \bar{q}_j)$ . Each of them are  $(n \times n)$ ,  $(k \times k)$  and  $(k \times n)$  matrices respectively. For  $n = N_F = 3$ , for example,  $\phi$  is the Goldstone boson nonet

$$\phi = \begin{pmatrix} \frac{\pi^0}{\sqrt{2}} + \frac{\eta}{\sqrt{6}} & \pi^+ & K^+ \\ \pi^- & -\frac{\pi^0}{\sqrt{2}} + \frac{\eta}{\sqrt{6}} & K^0 \\ K^- & \bar{K}^0 & -\frac{2\eta}{\sqrt{6}} \end{pmatrix} + \frac{\mathbf{1}}{\sqrt{3}}\eta'. \quad (2)$$

Under the chiral  $\text{SU}(n|k)_L \times \text{SU}(n|k)_R$ ,

$$\Sigma \rightarrow L \Sigma R^\dagger \quad (3)$$

where  $L \in \text{SU}(n|k)_L$ ,  $R \in \text{SU}(n|k)_R$ , and under charge conjugation  $C$ ,

$$C \Sigma C^{-1} = +\Sigma^\dagger. \quad (4)$$

The  $(n+k) \times (n+k)$  quark mass matrix is given by

$$\mathcal{M}_{ij} = \text{diag}(m_1, \dots, m_k, m_{k+1}, \dots, m_n; m_{k+1} \dots, m_n), \quad (5)$$

viz. the ghost quarks are degenerate in mass with  $k$ -flavors of the quarks. We also introduce

$$\mathcal{M}_\xi \equiv \frac{1}{2}(\xi^\dagger \mathcal{M} \xi^\dagger + \xi \mathcal{M} \xi). \quad (6)$$

Interactions among Goldstone boson fields are described by the chiral Lagrangian:

$$\begin{aligned} \mathcal{L} = & F_8(\text{Str} \ln \Sigma) \text{Str}(\partial_\mu \Sigma \partial^\mu \Sigma^\dagger) + F_0(\text{Str} \ln \Sigma) \text{Str}(\partial_\mu \ln \Sigma) \text{Str}(\partial^\mu \ln \Sigma^\dagger) \\ & + V_8(\text{Str} \ln \Sigma) \text{Str}(\mathcal{M}_\xi) + V_0(\text{Str} \ln \Sigma). \end{aligned} \quad (7)$$

Up to quadratic order in interactions [15],

$$\begin{aligned} F_8(\text{Str} \ln \Sigma) &= \frac{f^2}{8} + \dots \\ F_0(\text{Str} \ln \Sigma) &= \frac{A_0}{6} + \dots \\ V_8(\text{Str} \ln \Sigma) &= \frac{m_\pi^2 f^2}{4m_q} + \dots \\ V_0(\text{Str} \ln \Sigma) &= \frac{\mu_0^2 f^2}{24} (\text{Str} \ln \Sigma)(\text{Str} \ln \Sigma)^\dagger + \dots \end{aligned} \quad (8)$$

The main difference between quenched and unquenched QCD is the presence of  $F_0, V_0$  interactions that depend on  $\text{Str} \ln \Sigma$ . In unquenched QCD, this field corresponds to heavy  $\eta'$ -meson and decouples from low-energy dynamics. In quenched QCD, since the  $\eta'$ -meson remains light, their interactions has to be taken into account.

From the Lagrangian Eq.(7), one can obtain propagators of the Goldstone meson multiplets. Flavor-charged Goldstone mesons have the same kinetic terms, hence, propagator structures as those of full QCD. On the other hand, for the flavor-neutral Goldstone mesons, non-decoupling of  $\text{Str} \ln \Sigma$  field gives rise to non-standard form of the kinetic term. For simplicity, we will consider the ‘‘degenerate  $\text{SU}(n|k)$ -theory’’, where all the  $m_i (i = 1, \dots, n)$  masses are equal. In Euclidean momentum space, for  $\alpha = 0$ , the propagators of the flavor-neutral Goldstone bosons are given by

$$[G^{-1}]_{ij} = \delta_{ij} (p^2 + m_\pi^2) \epsilon_i + \frac{\mu_0^2}{3} \epsilon_i \epsilon_j. \quad (9)$$

(Non-zero  $A_0$  can be easily reinstated by shifting  $\mu_0^2 \rightarrow \mu_0^2 + A_0 p^2$ .) The grading index  $\epsilon_i$  is such that  $\epsilon(q_i) = +1, \epsilon(\tilde{q}_j) = -1$ . The corresponding propagator takes an extremely simple form

$$G_{ij} = \left[ \frac{\delta_{ij} \epsilon_i - 1/(n-k)}{p^2 + m_\pi^2} + \frac{1/(n-k)}{p^2 + m_\pi^2 + (n-k) \mu_0^2/3} \right]. \quad (10)$$

The propagator is a sum of two simple-pole contributions: one with equal mass to all meson multiplets and one with a shifted mass including the singlet contribution. Also note that, as  $n \rightarrow k$ , the shifted pole moves back to the pion pole. The propagator will then have a double pole at  $m_\pi^2$ , which is a well-known result in Q $\chi$ PT [14].

## 1.2 Vector Meson Multiplet Sector

Standard chiral perturbation theory for vector mesons has been formulated by Jenkins, Manohar and Wise in Ref. [29] and the quenched counterpart by Booth, Chiladze and Falk in Ref. [27]. Here we will construct the partially quenched theory.

Vector meson multiplet is described by  $(n+k) \times (n+k)$  graded matrix field, much the same way in structure as the Goldstone meson multiplet:

$$\mathcal{N}_\mu = \begin{pmatrix} \mathcal{V} & \psi \\ \psi^\dagger & \tilde{\mathcal{V}} \end{pmatrix}_\mu \quad (11)$$

where  $\mathcal{V}_\mu$  is the usual vector meson matrix field, which for  $n = N_F = 3$  is given by

$$\mathcal{V}_\mu = \begin{pmatrix} \frac{\rho^0}{\sqrt{2}} + \frac{\phi^8}{\sqrt{6}} & \rho^+ & K^{*+} \\ \rho^- & -\frac{\rho^0}{\sqrt{2}} + \frac{\phi^8}{\sqrt{6}} & K^{*0} \\ K^{*-} & \bar{K}^{*0} & -\frac{2\phi^8}{\sqrt{6}} \end{pmatrix}_\mu + \frac{\mathbf{I}}{\sqrt{3}} S_\mu \quad (12)$$

Under the  $[\text{SU}(n|k)_L \times \text{SU}(n|k)_R] \otimes \text{U}(1)$  graded chiral symmetry,

$$\mathcal{N}_\mu \rightarrow U \mathcal{N}_\mu U^\dagger \quad (13)$$

and under charge conjugation,

$$C \mathcal{N}_\mu C^{-1} = -\mathcal{N}_\mu^T. \quad (14)$$

We treat the vector meson multiplet as heavy, static source, which was previously utilized for conventional  $\chi$ PT for vector mesons [29] and for Q $\chi$ PT for vector mesons [27]. In this formalism, the static vector meson propagates with a fixed four-velocity  $v_\mu$ ,  $v^2 = 1$  and interacts with soft Goldstone multiplets. Three polarization states of vector mesons are perpendicular to the propagation direction, viz.  $v \cdot \mathcal{N} = 0$ . The chiral Lagrangian which describes the interactions of the vector meson multiplet with the soft Goldstone meson multiplet consists of three parts. At leading order in derivative and quark mass perturbations, they are

$$\mathcal{L}_V = \mathcal{L}_{\text{kin}} + \mathcal{L}_{\text{int}} + \mathcal{L}_{\text{mass}} \quad (15)$$

where

$$\mathcal{L}_{\text{kin}} = -i\text{Str}(\mathcal{N}_\mu^\dagger v \cdot \mathcal{D}\mathcal{N}_\mu) - iA_1(\text{Str}\mathcal{N}_\mu^\dagger)v \cdot \mathcal{D}(\text{Str}\mathcal{N}_\mu) \quad (16)$$

$$\mathcal{L}_{\text{mass}} = \bar{\mu}\text{Str}(\mathcal{N}_\mu^\dagger\mathcal{N}_\mu) + \mu_1(\text{Str}\mathcal{N}_\mu^\dagger)(\text{Str}\mathcal{N}_\mu) \quad (17)$$

$$+ \lambda_1\left((\text{Str}\mathcal{N}_\mu^\dagger)(\text{Str}\mathcal{N}_\mu\mathcal{M}_\xi) + \text{h.c.}\right) + \lambda_2\text{Str}(\{\mathcal{N}_\mu^\dagger, \mathcal{N}_\mu\}\mathcal{M}_\xi). \quad (18)$$

Here, covariant derivative is defined by

$$\mathcal{D}_\mu = \partial_\mu + [V^\mu, \ ] \quad (19)$$

and

$$V^\mu = \frac{1}{2}(\xi\partial^\mu\xi^\dagger + \xi^\dagger\partial^\mu\xi), \quad A^\mu = \frac{1}{2}(\xi\partial^\mu\xi^\dagger - \xi^\dagger\partial^\mu\xi). \quad (20)$$

The second terms in Eqs. (16, 17) are new interactions present in (partially) quenched QCD. The first term in Eq. (17) corresponds ‘residual mass’  $\bar{\mu}$  of vector meson multiplets. By a suitable reparametrization transformation [31], it is always possible to remove the residual mass. Using this freedom, we will choose  $\bar{\mu} = 0$  throughout this paper. The last two terms in Eq. (17) correspond to SU(3) isospin breaking due to quark masses. We will not use these terms in this paper.

The propagator of heavy vector mesons is similar to Goldstone meson multiplets. For flavor non-diagonal vector mesons, the propagator is

$$G_{\mu\nu}(k) = \Pi_{\mu\nu} \frac{1}{v \cdot k} \quad (21)$$

where  $k^\mu$  denotes residual momentum of vector meson and

$$\Pi_{\mu\nu} \equiv (v^\mu v^\nu - g^{\mu\nu}) \quad (22)$$

is the projection operator. For flavor-diagonal vector meson multiplets, the propagator is

$$G_{ij,\mu\nu}(k) = \Pi_{\mu\nu} \left[ \frac{\delta_{ij}\epsilon_i - 1/(n-k)}{v \cdot k} + \frac{1/(n-k)}{v \cdot k + (n-k)\mu_1} \right], \quad (23)$$

in which we have set  $A_1 = 0$ . Non-zero  $A_1$  can be incorporated by shifting  $\mu_1 \rightarrow \mu_1 + A_1 v \cdot k$ .

There are four-types of chiral invariant interactions between vector meson multiplets and Goldstone boson multiplets that are consistent with graded chiral symmetry:

$$\begin{aligned} \mathcal{L}_{\text{int}} = & ig_1(\text{Str}\mathcal{N}_\mu^\dagger)(\text{Str}\mathcal{N}_\nu A_\lambda)v_\sigma\epsilon^{\mu\nu\lambda\sigma} + \text{h.c.} \\ & + ig_2\text{Str}(\{\mathcal{N}_\mu^\dagger, \mathcal{N}_\nu\}A_\lambda)v_\sigma\epsilon^{\mu\nu\lambda\sigma} \\ & + ig_3(\text{Str}\mathcal{N}_\mu^\dagger)(\text{Str}\mathcal{N}_\nu)(\text{Str}A_\lambda)v_\sigma\epsilon^{\mu\nu\lambda\sigma} \\ & + ig_4\text{Str}(\mathcal{N}_\mu^\dagger\mathcal{N}_\nu)(\text{Str}A_\lambda)v_\sigma\epsilon^{\mu\nu\lambda\sigma}. \end{aligned} \quad (24)$$

## 2 Non-analytic Chiral Correction to Vector Meson Mass

To illustrate the application of PQ $\chi$ PT of vector mesons, we will calculate the mass correction of the  $\rho$  meson in PQ $\chi$ PT. The  $\rho$  meson mass is highly important in lattice calculation as it is often used to set the overall mass scale. The non-analytic correction to  $m_\rho$  in Q $\chi$ PT has been calculated in Ref. [27], where it is shown to be very different from its counterpart in the standard  $\chi$ PT [29, 27]. We will see below that in a sense the PQ $\chi$ PT result is intermediate between these two extreme cases.

### 2.1 Remarks on Parameters of PQ $\chi$ PT Lagrangian

The chiral one-loop corrections to  $\rho$ -meson mass come from the diagrams shown in Fig. 1. Fig. 1a is from the expansion of  $\mathcal{L}_{\text{kin}}$ . The resulting one-loop tadpole also contains both regular and hairpin insertion contributions. However, because the interaction vertex is proportional to the vector meson four-velocity  $v^\mu$ , this partially quenched one-loop tadpole contributes only to the wave function renormalization but not to the vector meson mass correction<sup>7</sup>. Such tadpole diagrams also comes from the quark mass matrix terms in the Lagrangian and in general may lead to non-trivial mass correction. However, we will be working in the degenerate mass limit, in which these tadpole diagrams do not contribute. Fig. 1b comes from the interaction Lagrangian Eq.(24) and depends on the values of  $g_{1,2,3,4}$ , as well as the hairpin parameters  $A_0, \mu_0^2$  in the Goldstone meson sector and  $A_1, \mu_1$  in the vector meson sector. Just as the coupling constants in normal  $\chi$ PT, they are undetermined parameters in the theory. To make the matter worse, the values of these parameters of PQ $\chi$ PT need not to be the same as those in QCD, and hence cannot be extracted from experimental data. In principle, one may be able to extract the value of these parameters from lattice simulation data, which may accumulate enough in the foreseeable future. Evidently it is difficult to extract any useful information from the theory with so many undetermined parameters. Because of this complication, we pick particular values for these parameters partly motivated by comparison with standard QCD chiral Lagrangian in the large  $N_c$  limit and hope that the set of values we picked is “generic”, viz. no accidental cancelation or enhancement takes place. In order to make our presentation as clear as possible, we restrict our investigation to the above truncated set of interactions and relegate a complete and detailed study retaining all the relevant couplings to a separate paper.

Since we are going to compare our results to the Q $\chi$ PT counterparts, we will choose the same hairpin parameters as adopted in Ref. [27], i.e.,  $A_1 = 0, \mu_1 = 0$ , while  $\mu_0^2/3 = (400\text{MeV})^2$

---

<sup>7</sup>This chiral one-loop contribution was not considered in [27].





Figure 1: Chiral one-loop diagrams to vector meson two-point function. Horizontal lines denote vector mesons and upper internal lines are Goldstone meson multiplets.

and  $A_0/3 = 0.2$ . Note that these choices are fundamentally arbitrary; there is no reason that the parameters have to have identical values in these two different theories, although this seems to be the most “natural” and “unbiased” choice and make comparison easy. We will also follow Ref. [27] in setting  $g_{3,4} = 0$  and  $g_2 = 0.75$ , the latter having the same value of the counterpart in normal  $\chi$ PT [29]. We emphasize again that there is *no* reason why we should set these coupling parameters the same between the two  $\chi$ PT’s. We have chosen to differ from Ref. [27] in setting  $g_1 = 0$  instead of 0.75. This choice is based on the observation that generically there will be interference terms proportional to  $g_1 g_2$ , hence, that the result will be highly sensitive to the *relative sign* between  $g_1$  and  $g_2$ , which is again theoretically undetermined. Since we have no way to discern whether the interference should be constructive or destructive, we will choose to set  $g_1 = 0$  in order to obtain *interference-independent predictions*. Again, we emphasize that this is an arbitrary choice of parameters. If desired, one can easily perform an analogous calculation with a different set of parameters. Nevertheless, we expect that this choice retains essential physics and that the results are at least qualitatively correct.

## 2.2 Chiral One-Loop Calculation

Now we are at the stage for the calculation of the chiral one-loop correction to the  $\rho$  meson mass in PQ $\chi$ PT. All the diagrams involved have the same one-loop Feynman integral structure<sup>8</sup> :

$$\mathcal{I}_1(m^2) = -\frac{1}{12\pi f^2} m^3. \quad (25)$$

For concreteness we will calculate the mass correction of a charged  $\rho$  meson. (The calculation would be somewhat more complicated with a neutral  $\rho$  meson, but because of the isospin

---

<sup>8</sup>Note that the same object is denoted as  $\mathcal{I}_1(m)$  in Ref. [27].

symmetry, the mass correction of all  $\rho$  mesons should be the same.) With the choice that only  $g_2 \neq 0$ , the ghost-antighost meson does not contribute, and there are four different types of contribution to the mass correction  $\Delta m_\rho$ :

(1) Intermediate Goldstone meson is quark-antighost or ghost-antiquark meson.

The contribution is given by

$$\Delta m_\rho = -g_2^2 \cdot 2k \cdot \mathcal{I}_1(m_\pi^2), \quad (26)$$

where the factor  $2k$  follows from the contraction of flavor indices.

(2) Intermediate Goldstone meson is flavor-charged (for  $n = 2$ ,  $u\bar{d} = \pi^+$  and  $d\bar{u} = \pi^-$ ).

The contribution is given by

$$\Delta m_\rho = +g_2^2 \cdot 2(n-1) \cdot \mathcal{I}_1(m_\pi^2). \quad (27)$$

(3) Intermediate Goldstone meson is flavor-neutral, (for  $n = 2$ ,  $u\bar{u}$  and  $d\bar{d}$ , which are linear combinations of  $\pi^0$  and  $\eta'$ ), and the propagator is given by the first term in Eq. (10).

The contribution is given by

$$\Delta m_\rho = +g_2^2 \cdot 2 \cdot \left(1 - \frac{2}{\Delta n}\right) \cdot \mathcal{I}_1(m_\pi^2). \quad (28)$$

where  $\Delta n \equiv (n - k)$ .

(4) Intermediate Goldstone meson is flavor-neutral, and the propagator is given by the second term in Eq. (10).

For this term the pole in the Goldstone boson propagator is shifted, and the contribution is given by

$$\Delta m_\rho = +g_2^2 \cdot 2 \cdot \left(\frac{2}{\Delta n}\right) \cdot \left(\frac{1}{1 + \Delta n \cdot A_0/3}\right) \cdot \mathcal{I}_1\left(\frac{m_\pi^2 + \Delta n \cdot \mu_0^2/3}{1 + \Delta n \cdot A_0/3}\right). \quad (29)$$

The total chiral one-loop correction is a sum of these four contributions:

$$\Delta m_\rho = 2g_2^2 \left[ \Delta n \mathcal{I}_1(m_\pi^2) - \frac{2}{\Delta n} \mathcal{I}_1(m_\pi^2) + \frac{2}{\Delta n} \left(\frac{1}{1 + \Delta n \cdot A_0/3}\right) \mathcal{I}_1\left(\frac{m_\pi^2 + \Delta n \cdot \mu_0^2/3}{1 + \Delta n \cdot A_0/3}\right) \right]. \quad (30)$$

Note that the final result depends only on  $\Delta n$ , which counts the difference in the number of quarks and the number of ghosts, but not  $n$  or  $k$  separately. Physically this reflects an obvious fact that physical quantities should be unchanged upon introduction of a degenerate set of extra quark and extra ghost, as their contribution should cancel out completely.

Finally, we note that our result can be expressed in terms of just  $\mathcal{I}_1$ , which also appears in the standard  $\chi$ PT result. (See below for a comparison between PQ $\chi$ PT and  $\chi$ PT results.) The “new chiral singularities” or “quenched infrared divergences” which appear in Q $\chi$ PT and are denoted by  $\mathcal{I}_{2,3,4}$  in Ref. [27], do not appear. This is in full agreement with the Bernard–Golterman’s third theorem [15], which states that *quenched infrared divergences appear if and only if one or more of the valence quarks are fully quenched*. Since the theory we are considering is only partially quenched, we do not see these new chiral singularities.

### 2.3 $\Delta n = 0$ Case – Fully Quenched QCD Limit

As mentioned above, partially quenched QCD was introduced to bridge between the two extreme cases, namely fully quenched and unquenched QCD theories. One would expect, by setting  $\Delta n = 0$ , the Q $\chi$ PT results should be recovered. In particular, the non-analytic quenched infrared singularities should reappear. Can we see this explicitly from our results?

The answer is a resounding yes. Let us see how this arises. Note that Eq. (30) can be re-expressed as

$$\Delta m_\rho = 2g_2^2 \left[ \Delta n \cdot \mathcal{I}_1(m_\pi^2) + \frac{2}{\Delta n} \cdot \left( \left( \frac{1}{1 + \Delta n A_0/3} \right) \mathcal{I}_1\left(\frac{m_\pi^2 + \Delta n \cdot \mu_0^2/3}{1 + \Delta n \cdot A_0/3}\right) - \mathcal{I}_1(m_\pi^2) \right) \right]. \quad (31)$$

When  $\Delta n \rightarrow 0$ , the first term vanishes while the second term becomes a derivative;

$$\Delta m_\rho = 4g_2^2 \frac{d}{d\Delta n} \left[ \frac{1}{1 + \Delta n \cdot A_0/3} \cdot \mathcal{I}_1\left(\frac{m_\pi^2 + \Delta n \cdot \mu_0^2/3}{1 + \Delta n \cdot A_0/3}\right) \right]_{\Delta n=0}. \quad (32)$$

Now it is clear how the Bernard–Golterman’s third theorem breaks down (as predicted by Bernard and Golterman) in the fully quenched limit. While the contributions from both the pion pole and the shifted pole are of the functional form  $\mathcal{I}_1$ , in the fully quenched limit the shifted pole returns back to its unshifted position and produces a derivative term which is *not* of the form  $\mathcal{I}_1$ . Expanding the derivative explicitly, one finds that

$$\begin{aligned} \mathcal{I}_2(m_\pi^2) &\equiv \frac{d}{d\Delta n} \left[ \frac{1}{1 + \Delta n \cdot A_0/3} \cdot \mathcal{I}_1\left(\frac{m_\pi^2 + \Delta n \cdot \mu_0^2/3}{1 + \Delta n \cdot A_0/3}\right) \right]_{\Delta n=0} \\ &= \frac{1}{12\pi f^2} \left( \frac{3}{2} \cdot \frac{\mu_0^2}{3} m_\pi - \frac{5}{2} \cdot \frac{A_0}{3} \cdot m_\pi^3 \right), \end{aligned} \quad (33)$$

and the term linear in  $m_\pi$  is the anticipated non-analytic quenched infrared singularity. The mass correction in the fully quenched limit is

$$\Delta m_\rho = 4 g_2^2 \mathcal{I}_2(m_\pi^2), \quad (34)$$

which agrees perfectly with Eq. (3.23) of Ref. [27]<sup>9</sup>. We thus have established that PQ $\chi$ PT does reproduce Q $\chi$ PT results in the fully quenched limit  $\Delta n = 0$ .

## 2.4 $k = 0$ Case – Unquenched Limit

Let's now turn our attention to the other end of the limits. Does it reproduce the standard  $\chi$ PT results in the unquenched limit  $k = 0$ ?

This time the answer is clearly no! In normal  $n = 2$   $\chi$ PT, we have only pion loops and hence do not expect a contribution from a shifted pole. In fact, the  $\chi$ PT result is straightforwardly calculated to be

$$\Delta m_\rho = g_2^2 \left(2n - \frac{4}{n}\right) \mathcal{I}_1(m_\pi^2) \quad (35)$$

which, as expected, does not contain any contribution from a shifted pole. So the question is, why have we failed to reproduce the unquenched QCD results?

This puzzle will be resolved by noting how we have obtained the  $\chi$ PT result quoted above. Let's imagine a world in which  $\eta'$  is degenerate with all the other Goldstone bosons (for example,  $N_c \rightarrow \infty$  world). The mass correction comes from Feynman diagram in Fig. 1b, and each diagram gives rise to a mass correction  $g_2^2 \cdot \mathcal{I}_1(m_\pi^2)$ . In each diagram we have an internal quark loop, which can take  $n$  flavors and 2 orientations (clockwise/anticlockwise), so there are in total  $2n$  diagrams. So naively one would expect  $\Delta m_\rho = g_2^2 \cdot 2n \cdot \mathcal{I}_1(m_\pi^2)$ . But this is not what we get from  $\chi$ PT, as this naive result includes contribution from  $\eta'$  loops, which has been integrated out in the standard  $\chi$ PT [29]. It is not difficult to see that the  $\rho\rho\eta'$  coupling is  $2g_2/\sqrt{n}$ , so the  $\eta'$  contribution is  $g_2^2(4/n)\mathcal{I}_1(m_\pi^2)$ . Result (35) is obtained exactly when the  $\eta'$  contribution is subtracted from the naive result.

Indeed, Eq. (35) agrees with the  $n = 2$  result [27],

$$\Delta m_\rho = g_2^2 \cdot 2 \cdot \mathcal{I}_1(m_\pi^2) \quad (36)$$

and the  $n = 3$  result [27, 29]

$$\Delta m_\rho = g_2^2 \left(2 \mathcal{I}_1(m_\pi^2) + 2 \mathcal{I}_1(m_K^2) + \frac{2}{3} \mathcal{I}_1(m_\eta^2)\right) = g_2^2 \cdot \frac{14}{3} \cdot \mathcal{I}_1(m_\pi^2) \quad \text{when } m_\pi = m_K = m_\eta. \quad (37)$$

---

<sup>9</sup>Note that  $M_0^2$  and  $A_0$  in Ref. [27] are our  $\mu_0^2/3$  and  $A_0/3$  respectively. Also recall that we have kept  $g_2$  as the only non-vanishing coupling.

It also reproduces exactly the  $\mathcal{I}_1(m_\pi^2)$  term in Eq. (30). Now it becomes clear what the remaining contribution from the shifted pole means physically: it is the reinstatement of  $\eta'$  contribution, and the shifting of the pole just reflects that, in the real world, the  $\eta'$  mass is shifted with respect to the pion mass due to the necklace diagrams. In other words, we can rearrange Eq. (30) in the following way,

$$\Delta m_\rho = g_2^2 \left(2n - \frac{4}{n}\right) \mathcal{I}_1(m_\pi^2) + g_{\rho\rho\eta'}^2 \mathcal{I}_1(m_{\eta'}^2), \quad (38)$$

where

$$g_{\rho\rho\eta'}^2 = 4g_2^2/Zn, \quad m_{\eta'}^2 = (m_\pi^2 + n\mu^2/3)/Z, \quad \text{where} \quad Z = (1 + n A_0/3), \quad (39)$$

which are the coupling, mass and wavefunction renormalization of the  $\eta'$  meson. Being organized this way, the first term of Eq.(38) exhibits exactly of the same functional form as the standard  $\chi$ PT result. Note that numerical value of respective coupling parameter  $g_2$  in PQ $\chi$ PT and in standard  $\chi$ PT differ generically each other. If the  $\eta'$  meson were integrated out instead of being truncated, its effect will be reflected to finite additive renormalization of the coupling parameters so that their values for PQ $\chi$ PT becomes numerically identical to those of  $\chi$ PT.

It is of interest to compare the above result with the Bernard-Golterman's first theorem. According to the theorem, *in the subsector where all valence quarks are unquenched, the  $SU(n|k)$  theory is completely equivalent to a normal, completely unquenched  $SU(n - k|0)$  theory*. We found that this is indeed true except that, compared to standard  $\chi$ PT, this “completely unquenched  $SU(n - k|0)$  theory” retains an  $\eta'$  meson which may (and does) contribute to chiral loop corrections. In fact, Bernard and Golterman [15] have already noted this aspect from their study of chiral perturbation theory for pion self-energy correction. In a low-energy effective theory, when treating not-so-heavy field excitations, one may either retain them or integrate out. As such, it should be viewed as a matter of choice whether one includes the  $\eta'$  in the effective theory. As with Bernard and Golterman, we have noted that effective theory of unquenched  $SU(n - k|0)$  theory is the one which retains  $\eta'$  explicitly. It should then be straightforward to identify Goldstone meson and  $\eta'$  contributions separately in a physical quantity, as is exemplified from the above calculation.

## 2.5 Numerical Comparison

To conclude this section, we provide plots of  $\Delta m_\rho$  as a function of pion mass in the following theories in Fig. 2. Recall that we have chosen the quenching parameters as  $A_0/3 = 0.2$  and  $\mu_0^2/3 = (400 \text{ MeV})^2$ .

- 0) Standard  $n = N_F = 2$   $\chi$ PT,

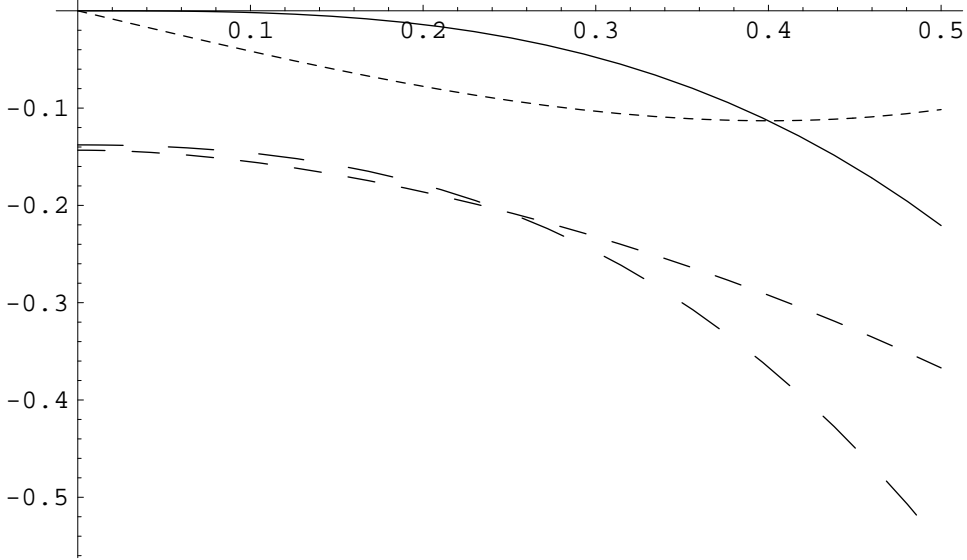


Figure 2: Chiral one-loop correction  $\Delta m_\rho$  (in unit of GeV) as a function of pion mass in the range (0, 0.5) GeV. Solid line is the standard QCD, small dashed line is the (2,2) theory, medium dashed line is the (2,1) theory and large-dashed line is the (2,0) theory.

- 1) PQ $\chi$ PT with  $(n, k) = (2, 0)$ , which is identical with  $\chi$ PT with  $\eta'$  contribution,
- 2) PQ $\chi$ PT with  $(n, k) = (2, 1)$ ,
- 3) PQ $\chi$ PT with  $(n, k) = (2, 2)$ , which is identical with Q $\chi$ PT.

From the plot it is clear that PQ $\chi$ PT is qualitative different from both  $\chi$ PT and Q $\chi$ PT. In both  $\chi$ PT and Q $\chi$ PT  $\Delta m_\rho$  vanishes in the chiral limit, while it is not the case for PQ $\chi$ PT. In fact, from Eq. (30) in the chiral limit, we find

$$\Delta m_\rho \Big|_{m_\pi^2=0} = \frac{4g_2^2}{\Delta n} \cdot \left( \frac{1}{1 + \Delta n \cdot A_0/3} \right) \cdot \mathcal{I}_1 \left( \frac{\Delta n \cdot \mu_0^2/3}{1 + \Delta n \cdot A_0/3} \right). \quad (40)$$

As mentioned in the previous sections, this contribution arises from heavy  $\eta'$  loops, which could have been integrated out of the low energy effective theory to recapture the correct chiral limit of  $\Delta m_\rho$ . By integrating out the  $\eta'$  meson in PQ $\chi$ PT, parameters in the Lagrangian are renormalized, the details of which are beyond the scope of the present study. In order to probe  $\eta'$  meson chiral loop correction and its pion mass dependence, we have subtracted  $\Delta m_\rho|_{m_\pi^2=0}$  from Eq.(30). The corrected plots are shown in Fig. 3 *assuming* tacitly that respective couplings are all the same. It is clearly verified, in the chiral limit, that PQ $\chi$ PT does behave as a continuous interpolation between  $\chi$ PT and Q $\chi$ PT as expected. It should be emphasized again that, should we subtract the  $\eta'$  contribution for a given pion mass, the PQ $\chi$ PT and  $\chi$ PT agree perfectly each other, as discussed in detail in the previous subsection. Thus, the difference between the

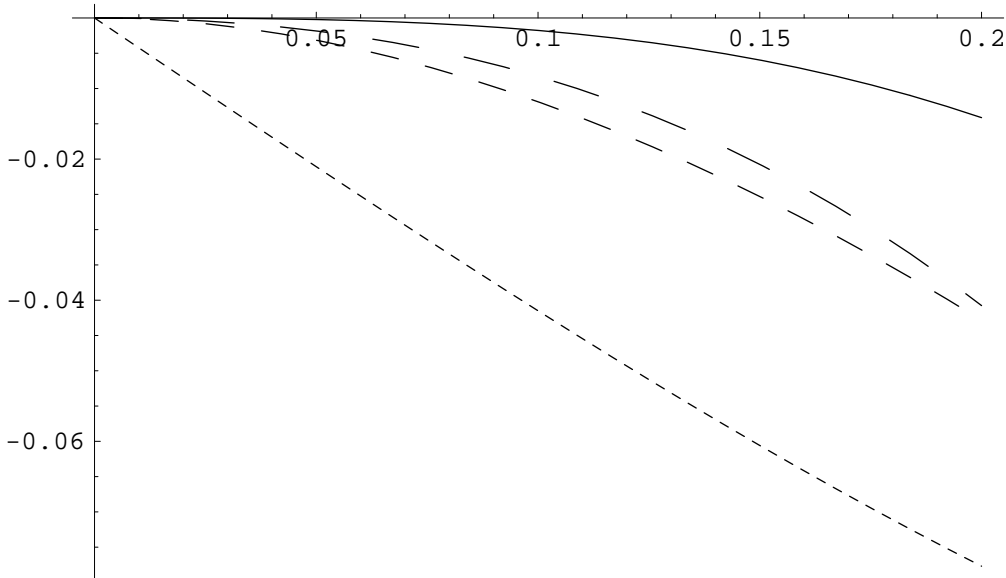


Figure 3:  $(\Delta m_\rho - \Delta m_\rho|_{m_\pi=0})$  in unit of GeV as a function of pion mass in the range  $(0, 0.2)$  GeV. Solid line is the standard QCD, small dashed line is the (2,2) theory, medium dashed line is the (2,1) theory and large-dashed line is the (2,0) theory.

solid and the large-dashed lines reflects dependence of the chiral correction due to  $\eta'$  meson to the pion mass.

### 3 Partially Quenched QCD and Tensor Mesons

In Ref. [30]  $\chi$ PT for tensor mesons have been developed. It has been found that  $\chi$ PT for tensor mesons is very similar to the vector meson counterpart, the only difference being the extra Lorentz indices contracted trivially. This is the reflection of decoupling from the dynamics of spin and flavor quantum numbers manifest in the heavy mass formalism that we have adopted for describing these mesons. This observation applies equally well to  $Q\chi$ PT and  $PQ\chi$ PT, as the Lorentz structure of these theories are identical with that in  $\chi$ PT. For completeness, we will formally write down  $PQ\chi$ PT for tensor mesons. The  $Q\chi$ PT can be recovered by setting  $n = k$ .

### 3.1 PQ $\chi$ PT for Tensor Mesons

Tensor meson multiplet is again described by  $(n+k)\times(n+k)$  graded matrix field in exactly the same manner as Goldstone meson and vector meson multiplets:

$$\mathcal{N}_{\mu\nu} = \begin{pmatrix} \mathcal{V} & \psi \\ \psi^\dagger & \tilde{\mathcal{V}} \end{pmatrix}_{\mu\nu}. \quad (1)$$

For the multiplets, we use the same symbol as the vector meson multiplet. This should not cause any confusion: spin of the multiplet is easily identified with the Lorentz indices. In Eq. (1),  $\mathcal{V}_{\mu\nu}$  denotes the usual tensor meson field, which for  $n = N_F = 3$  is given by

$$\mathcal{V}_{\mu\nu} = \begin{pmatrix} \frac{a_2^0}{\sqrt{2}} + \frac{f_2^{(8)}}{\sqrt{6}} & a_2^+ & K_2^{*+} \\ a_2^- & -\frac{a_2^0}{\sqrt{2}} + \frac{f_2^{(0)}}{\sqrt{6}} & K_2^{*0} \\ K_-^{*2} & \overline{K}_2^{*0} & -\frac{2f_2^{(8)}}{\sqrt{6}} \end{pmatrix}_{\mu\nu} + \frac{\mathbf{I}}{\sqrt{3}} f_2^{(0)}. \quad (2)$$

Under the  $[\text{SU}(n|k)_L \times \text{SU}(n|k)_R] \otimes \text{U}(1)$  graded chiral symmetry

$$\mathcal{N}_{\mu\nu} \rightarrow U \mathcal{N}_{\mu\nu} U^\dagger \quad (3)$$

and under charge conjugation,

$$C \mathcal{N}_{\mu\nu} C^{-1} = +\mathcal{N}_{\mu\nu}^T. \quad (4)$$

Following the construction developed in Ref. [30], we treat the static tensor mesons as propagating with a fixed four-velocity  $v_\mu$ ,  $v^2 = 1$  and as interacting with soft Goldstone meson multiplet along the trajectory. By definition, these tensor mesons are symmetric and traceless in Lorentz indices:

$$\mathcal{N}_{\mu\nu} = \mathcal{N}_{\nu\mu}, \quad \mathcal{N}_\mu^\mu = 0. \quad (5)$$

Moreover, the polarizations of the tensor mesons are necessarily orthogonal to the momentum, hence,

$$v^\mu \mathcal{N}_{\mu\nu} = 0. \quad (6)$$

The chiral Lagrangian density which described the interactions of the tensor meson multiplet with the low-momentum Goldstone meson multiplet has the same structure as the vector meson multiplet case:

$$\mathcal{L}_T = \mathcal{L}_{\text{kin}} + \mathcal{L}_{\text{mass}} + \mathcal{L}_{\text{int}}. \quad (7)$$

At leading order in the derivative and quark mass expansions and in Euclidean space,

$$\mathcal{L}_{\text{kin}} = -\frac{i}{2} \text{Str}(\mathcal{N}_{\mu\nu}^\dagger v \cdot \mathcal{D} \mathcal{N}_{\mu\nu}) - \frac{i}{2} A_2 (\text{Str} \mathcal{N}_{\mu\nu}^\dagger) v \cdot \mathcal{D} (\text{Str} \mathcal{N}_{\mu\nu})$$



$$\begin{aligned}
\mathcal{L}_{\text{mass}} &= \frac{\bar{\mu}_2}{2} \text{Str}(\mathcal{N}_{\mu\nu}^\dagger \mathcal{N}_{\mu\nu}) + \frac{\tilde{\mu}_2}{2} (\text{Str} \mathcal{N}_{\mu\nu}^\dagger) (\text{Str} \mathcal{N}_{\mu\nu}) \\
&+ \frac{\tilde{\lambda}_1}{2} \left( (\text{Str} \mathcal{N}_{\mu\nu}^\dagger) (\text{Str} \mathcal{N}_{\mu\nu} \mathcal{M}_\xi) + \text{h.c.} \right) + \frac{\tilde{\lambda}_2}{2} \text{Str}(\{\mathcal{N}_{\mu\nu}^\dagger, \mathcal{N}_{\mu\nu}\} \mathcal{M}_\xi). \tag{8}
\end{aligned}$$

As in the vector meson multiplet, we turn off isospin breaking quark mass perturbations and set the ‘residual mass’  $\bar{\mu}_2 = 0$ .

In terms of tensor projection operator

$$\Pi^{\mu\nu, \alpha\beta} \equiv (v^\mu v^\nu - g^{\mu\nu})(v^\alpha v^\beta - g^{\alpha\beta}) + \text{permutations}, \tag{9}$$

the tensor meson multiplet propagators are expressed as

$$G_{\mu\nu, \alpha\beta}(k) = \Pi_{\mu\nu\alpha\beta} \frac{1}{v \cdot k} \tag{10}$$

for flavor non-diagonal tensor meson multiplets, and

$$G_{\mu\nu, \alpha\beta}^{ij}(k) = \Pi_{\mu\nu\alpha\beta} \left[ \frac{\delta_{ij} \epsilon_i - 1/(n-k)}{v \cdot k} + \frac{1/(n-k)}{v \cdot k + (n-k)\mu_2} \right] \tag{11}$$

for flavor-diagonal multiplets. Again, in Eqs. (10, 23), we have set  $A_2 = 0$ . Non-zero  $A_2$  is reinstated by shifting  $\mu_2 \rightarrow \mu_2 + A_2 v \cdot k$ .

The chiral invariant interactions between tensor meson multiplets and Goldstone meson multiplets is essentially the same form as those of vector meson multiplets except contractions of Lorentz indices:

$$\begin{aligned}
\mathcal{L}_{\text{int}} &= i \frac{\tilde{g}_1}{2} (\text{Str} \mathcal{N}_{\mu\alpha}^\dagger) (\text{Str} \mathcal{N}_{\nu\alpha} A_\lambda) v_\sigma \epsilon^{\mu\nu\lambda\sigma} + \text{h.c.} \\
&+ i \frac{\tilde{g}_2}{2} \text{Str}(\{\mathcal{N}_{\mu\alpha}^\dagger, \mathcal{N}_{\nu\alpha}\} A_\lambda) v_\sigma \epsilon^{\mu\nu\lambda\sigma} \\
&+ i \frac{\tilde{g}_3}{2} (\text{Str} \mathcal{N}_{\mu\alpha}^\dagger) (\text{Str} \mathcal{N}_{\nu\alpha}) (\text{Str} A_\lambda) v_\sigma \epsilon^{\mu\nu\lambda\sigma} \\
&+ i \frac{\tilde{g}_4}{2} \text{Str}(\mathcal{N}_{\mu\alpha}^\dagger \mathcal{N}_{\mu\alpha}) (\text{Str} A_\lambda) v_\sigma \epsilon^{\mu\nu\lambda\sigma}. \tag{12}
\end{aligned}$$

Generalization to higher spin tensor meson multiplet is completely straightforward and is left as an exercise to the reader.

### 3.2 Chiral One-Loop Mass Correction to Tensor Mesons

From the construction above, it should be evident that the flavor structure decouples completely from the Lorentz spin structure in both the vector and the tensor case. Moreover, while tensor

meson fields carry one more Lorentz index than vector meson fields, the extra Lorentz indices are always contracted trivially in the Lagrangian. This has led us to an interesting observation in Ref. [30] that mass corrections due to 1-loop effects in  $\chi$ PT for tensor mesons is proportional to their counterparts for vector mesons, *up to numerical equality of the respective coupling constants*. Utilizing non-relativistic quark model, which is expected to be valid in large  $N_c$  limit, the proportionality constant has been calculated in Ref. [30] to be  $3/2$ . Since both the decoupling of flavor and Lorentz structures and the trivial contraction of additional Lorentz indices also continues to hold true for (P)Q $\chi$ PT, the proportionality result is also valid for (P)Q $\chi$ PT. We will state the result explicitly below:

**Proposition:** *In non-relativistic quark model, which is expected to be a good approximation in large  $N_c$  limit, chiral 1-loop corrections PQ $\chi$ PT to tensor meson masses are  $3/2$  times their counterparts in the vector meson masses, with all the coupling constants and hairpin parameters replaced by the corresponding parameters in the tensor meson Lagrangian. This result continues to hold in both the fully quenched and the completely unquenched limit.*

If one assumes the parameters in the vector and tensor meson chiral Lagrangians are the same, which we have argued to be a reasonable approximation in *non-relativistic quark model at large  $N_c$  limit*, we deduce the following relation valid at chiral one-loop order

$$\Delta m_{a_2} = \frac{3}{2} \Delta m_\rho. \quad (13)$$

This observation entails an interesting consequence. In quenched lattice QCD calculations, when extracting light hadron spectrum, physical mass scale is conveniently normalized by identifying  $\rho$ -meson pole on the lattice with physical  $\rho$ -meson mass. However, we have seen that vector meson mass is plagued by quenched chiral logarithms in the chiral limit. As such, it should be more desirable to use a combination of physical parameters that is insensitive to the quenched approximation. From the analysis above and Eq. (13), we expect quenched infrared divergences to be small for the combination  $(m_{a_2} - \frac{3}{2}m_\rho)$ , and one may consider using this combination to set the mass scale in lattice calculation<sup>10</sup>. In non-relativistic approach to lattice QCD [32], the physical mass scale is normalized by identifying S- and P-wave charmonium mass splitting on the lattice with its Particle Data Group value. It has been noted that this choice is quite insensitive to the quenching effect. We suspect that the underlying reason is similar to our proposal given above: for heavy charmonium, spin and flavor decouples from the dynamics and both S- and P-wave charmonium should receive similar chiral corrections.

---

<sup>10</sup>However, this will become practical only when the statistical uncertainties in the determination of tensor mesons is as small as those of vector mesons.

## 4 Discussions

In this paper, we have developed quenched and partially quenched chiral perturbation theory for vector and tensor mesons. We have formulated the quenched Lagrangian, and evaluated the chiral correction to  $m_\rho$  under a specific choice of parameters that are partly motivated by large- $N_c$  limit. While the formal expression of  $\Delta m_\rho$  may be modified if one also includes the effects of the hairpin parameters of the singlet vector meson and/or the  $g_{1,3,4}$  couplings, we expect our analysis has captured the generic qualitative feature of PQ $\chi$ PT. Just as the essential new physics (when compared to standard unquenched  $\chi$ PT) of Q $\chi$ PT is the double pole in the singlet meson propagators, the essential new physics of PQ $\chi$ PT is the shifted pole, which is carefully studied in this paper. Through this study we have clarified the connection between PQ $\chi$ PT to its two extreme limits: Q $\chi$ PT and standard  $\chi$ PT. We have clarified that, in the fully quenched limit, how the quenched infrared divergences arises through the incomplete cancellation of the pion pole and the shifted pole. We have also shown that the unquenched limit of PQ $\chi$ PT is not, as naively expected, standard  $\chi$ PT, but  $\chi$ PT with the  $\eta'$  meson. What we have achieved is an intrapolation between  $\chi$ PT and Q $\chi$ PT, which was one of the motivations behind Bernard and Golterman's original invention of partially quenched QCD.

In our treatment of the vector and tensor meson fields we have adopted the heavy particle formalism, which has now become a standard technique in the treatment of matter fields in chiral perturbation theory. By using the heavy particle formalism one has excluded the effects of heavy particle number violating processes like  $\rho \rightarrow \pi\pi \rightarrow \rho$ , which is not captured in our Lagrangian. One may wonder if this would lead to substantial corrections to our results. Through a model calculation, this issue has been addressed in Ref. [33], where it has been found that the effect of heavy particle number violating processes is negligibly small. This problem may be more severe for tensor mesons, but so far no reliable estimate has been made on these corrections. On the other hand, more relevant to the present study, there are also  $1/M$  correction due to the finite masses of the vector and tensor mesons under study. The tensor mesons ( $M \sim 1.4$  GeV) are probably heavy enough (note that  $\chi$ PT works well for the N- $\Delta$  system with  $M \sim 1$  GeV). The vector mesons are not that heavy at all, and there may be sizable  $1/M$  corrections, especially, when one has to couple the  $\rho$  meson ( $m_\rho = 0.770$  GeV) to the  $\eta'$  meson ( $m_{\eta'} = 0.958$  GeV). It is evident that more studies on these corrections would provide invaluable information to our understanding of quenched and partially quenched QCD.

We thank M. Alford, C. Bernard, P. Lepage, C. Michael, S. Sharpe and F. Wilczek for useful discussions and correspondences and C. Bernard for careful reading of the manuscript and invaluable comments.

## References

- [1] D. Weingarten, Phys. Lett. **109B** (1982) 57;  
H. Hamber and G. Parisi, Phys. Rev. Lett. **47** (1981) 1792.
- [2] T. Bhattacharya, R. Gupta, G. Kilcup and S.R. Sharpe, Phys. Rev. **D53** (1996) 6486.
- [3] C. Bernard *et.al.* (MILC Collaboration), Nucl. Phys. **53** [Proc. Suppl.] (1997) 212.
- [4] R. Kenway *et.al.* (UKQCD Collaboration), Nucl. Phys. **53** [Proc. Suppl.] (1997) 206.
- [5] S. Aoki *et.al.* (JLQCD Collaboration), Nucl. Phys. **53** [Proc. Suppl.] (1997) 209.
- [6] U. Glaessner *et.al.* (SESAM Collaboration), Nucl. Phys. **53** [Proc. Suppl.] (1997) 219.
- [7] For a review, see S. Gottlieb, Nucl. Phys. **53** [Proc. Suppl.] (1997) 155.
- [8] T. A. DeGrand and M. W. Hecht, Phys. Rev. **D46** (1992) 3937.
- [9] P. Lacock, C. Michael, P. Boyle and P. Rawland, Phys. Rev. **D54** (1996) 6997; Phys. Lett. **B401** (1997) 308.
- [10] C. Bernard *et.al.*(MILC Collaboration), *Exotic Mesons in Quenched Lattice QCD* ,  
hep-lat/9707008 .
- [11] H.D. Politzer, Phys. Lett. **116B** (1982) 171.
- [12] S.R. Sharpe, Phys. Rev. **D41** (1990) 3233.
- [13] S.R. Sharpe, Phys. Rev. **D46** (1992) 3146.
- [14] C.W. Bernard and M.F. Golterman, Phys. Rev. **D46** (1992) 853.
- [15] C.W. Bernard and M.F. Golterman, Phys. Rev. **D49** (1994) 486.
- [16] R. Gupta, Nucl. Phys. **42** [Proc. Suppl.] (1994) 85.
- [17] S. Kim and D.K. Sinclair, Phys. Rev. **D52** (1995) 2614.
- [18] P. Lacock and C. Michael (UKQCD Collaboration), Phys. Rev. **D52** (1995) 5213.
- [19] S.R. Sharpe, Nucl. Phys. [Proc.Suppl.] **53** (1997) 181.
- [20] M.F. Golterman, *Chiral Perturbation Theory and the Quenched Approximation of QCD*,  
hep-lat/9411005 .

- [21] A. Morel, *J. Physique (Paris)* **48** (1987) 111.
- [22] G.M. de Divitiis, R. Frezzotti, M. Masetti and R. Petronzio, *Phys. Lett.* **387B** (1996) 829.
- [23] S.R. Sharpe, *Enhanced Chiral Logarithms in Partially Quenched QCD*, hep-lat/9707018.
- [24] J.N. Labrenz and S.R. Sharpe, *Phys. Rev.* **D54** (1996) 4595.
- [25] M. Booth, *Phys. Rev.* **D51** (1995) 2338;  
S.R. Sharpe and Y. Zhang, *Phys. Rev.* **D53** (1996) 5125.
- [26] W. Bardeen, A. Dunca, E. Eichten and H. Thacker, *Quenched Approximation Artifacts: A Detailed Study in Two-Dimensional QED*, hep-lat/9705002.
- [27] M. Booth, G. Chiladze and A.F. Falk. *Phys. Rev.* **D55** (1997) 3092.
- [28] J. Gasser and H. Leutwyler, *Nucl. Phys.* **B250** (1985) 465.
- [29] E. Jenkins, A.V. Manohar and M.B. Wise, *Phys. Rev. Lett.* **75** (1995) 2272.
- [30] C.K. Chow and S.J. Rey, *Chiral Perturbation Theory for Tensor Mesons*, hep-ph/9708355.
- [31] A. Falk, M. Neubert and M. Luke, *Nucl. Phys.* **B388** (1992) 363.
- [32] C.T.H. Davies *et.al.* (NRQCD Collaboration), *Phys. Rev.* **D50** (1994) 6963; *Phys. Rev.* **D52** (1995) 6519; *Phys. Lett.* **B382** (1996) 131.
- [33] D.B. Leinweber and T.D. Cohen, *Phys. Rev.* **D49** (1994) 3512.